JOURNAL OF MECHANICAL ENGINEERING AND SCIENCES (JMES)
ISSN: 2289-4659 e-ISSN: 2231-8380
VOL. 16, ISSUE 1, 8673 – 8690
DOI: https://doi.org/10.15282/jmes.16.1.2022.03.0686

ORIGINAL ARTICLE

Numerical analysis of wake turbulence between hybrid tidal turbine and hypothetical actuator cylinder for shallow water with low velocity conditions

L. Dass, A. A. Rahman*, K. Rajendran, G. E. Suhri

Faculty of Mechanical Engineering Technology, Universiti Malaysia Perlis, Pauh Putra Main Campus, 02600 Arau, Perlis, Malaysia.
Phone: +6049885035; Fax: +6049885034

ABSTRACT – Towards modernisation of the technological era, electricity demands have been an issue. Although the supply of electrical energy from the renewable sources are increasing, it is still not sufficient to offset the carbon production. Malaysia as a developing country needs ample of supply of electrical energy. As most of the current electrical energy for the country are being produced by non renewable sources, the Malaysian government have started looking into renewable options to produce electrical energy. There are various sources of energy that are available in Malaysia such as solar, natural gas, petroleum, ocean energy and many more. This paper is focused on the tidal energy which is an ocean energy that can produce electrical energy by using the power of tide. This research explores the hybrid turbine design which is a type of vertical-axis tidal turbine that combines two distinct type of devices, namely Savonius and H-Darrieus turbines. Hybrid turbine is useful as it helps to overcome the limitation of individual turbine and also be able to produce energy at a low water velocity. Numerical analysis is employed to investigate the wake recovery behaviour and turbulent mixing due to the positioning of the device using Ansys CFD Fluent. By understanding the general wake characteristics produced by each device, proper planning can be done to configure these devices in an array for future planning. The simulation result shows that the hybrid turbine utilising NACA0015 and NACA0018 with nested configuration demonstrates faster velocity recovery compared to NACA0021. The turbulence wake results also provides a promising output which shows the acceleration of flow at the downstream region for hybrid nested NACA0015 and NACA0018 are more narrow compared to NACA0021. The result of this simulation has also been validated with published data. In a nutshell, the NACA blade design not only affects the performance of the turbine but can also influence the velocity recovery downstream of the device.

ARTICLE HISTORY
Received: 14th Sept. 2021
Revised: 25th Oct. 2021
Accepted: 03rd Dec. 2021

KEYWORDS
vertical turbine;
hydrodynamics;
nested turbine;
marine energy;
velocity recovery

INTRODUCTION

Electricity is one of the primary sources of energy that is important to humankind. However, for years the consumption of electricity worldwide has increased dramatically [1]. For a developing country such as Malaysia, the demand for electrical energy will keep on growing. Since 80% of Malaysia's power are generated from a non-renewable source such as coal and natural gas [2], the Malaysian government has been directing their interest and focus on renewable energy research.

There are a few renewable energies that are available in the country. Most of them are generated from photovoltaics which is the highest contribution of the renewable energy mix. The downside of solar energy is that it needs solar radiation to produce electricity and solar radiation is not available 24 hours of the time. This is why this paper is more focused on ocean renewable energies, specifically tidal energy. Tidal energy is a source of energy that is generated from the gravitational effect of the sun and the moon. Since tides are a phenomenon that is very predictable and continuous, tidal energy has a great future in the renewable energy sector. On account of the tidal forces, there are three types of tidal cycles, particularly Semi-diurnal, Mixed and Diurnal. The formation of these cycles is highly dependent on the position of the moon and sun [3].

In the tidal energy industry, several technologies can be used to harness the kinetic energy produced by the movement of water, for instance, dynamic tidal power, tidal lagoon, tidal barrage, and tidal turbine [3]. A tidal turbine is a technology that closely resembles wind turbine technology. The major difference between the two technologies is that the density of the fluid used and the environment. Horizontal Axis Tidal Turbine (HATT) and Vertical Axis Tidal Turbine (VATT) are two major turbine designs that are employed to harness the kinetic energy from the tide for specific applications. Since HATT has proven to be more efficient in deep water tidal harnessing, many studies in the European region are concentrated on the HATT design. As for VATT design, this turbine's technological advancement is not yet matured compared to HATT because VATT is mainly deployed for shallow depth areas. Nonetheless, as VATT is a bi-directional turbine, it can rotate at any flow direction. It does not need an extra tool to navigate the blades towards the water flow direction [4]. Since Malaysia's open water can be categorised as shallow, this study will concentrate on the VATT design for use in shallow water conditions [5].

*CORRESPONDING AUTHOR | A.A. Rahman | ✉ anasrahman@unimap.edu.my

A nested turbine or a hybrid turbine is a type of VATT design that consists of two standalone turbines, which are H-Darrieus and Savonius turbines. This combination of two VATT devices is designed to overcome each of the turbines' limitations. Savonius is known for its low efficiency while H-Darrieus is known for its low starting speed. Another challenge for this standalone turbine design is that it can lower the upstream velocity significantly after passing by the turbine [4]. A nested turbine is also known as a low-speed current turbine since it can generate power from a relatively slow-moving flow. Correspondingly, since the average current flow for Malaysia's open water is about 0.6m/s [6], a nested turbine is the ideal turbine choice to be implemented for possible energy extraction from the tides.

This paper aims to provide an understanding of the design of a nested hybrid turbine that can influence the wake and the velocity recovery of the device in shallow and low-speed water conditions. Additionally, this paper also would like to explore the difference in the turbulent wake characteristics between the hybrid nested turbine and hypothetical cylinder which is used as a representation of a standalone turbine.

Darrieus Turbine

Darrieus turbine is a vertical type of turbine which utilises the lift force acting on the airfoil blades. The Darrieus will rotate opposite to the fluid direction which will generate aerodynamic force. There are few types of Darrieus turbines which are Phi rotor, J-Darrieus , Helical Darrieus and H-Darrieus. By looking at all their advantages and disadvantages, H-Darriues turbine design is the best option to be used in this hybrid nested turbine because of its simple design and having a low manufacturing cost compared to the other Darrieus turbines [7, 8]. Figure 1 shows the working principle of H-Darrieus.

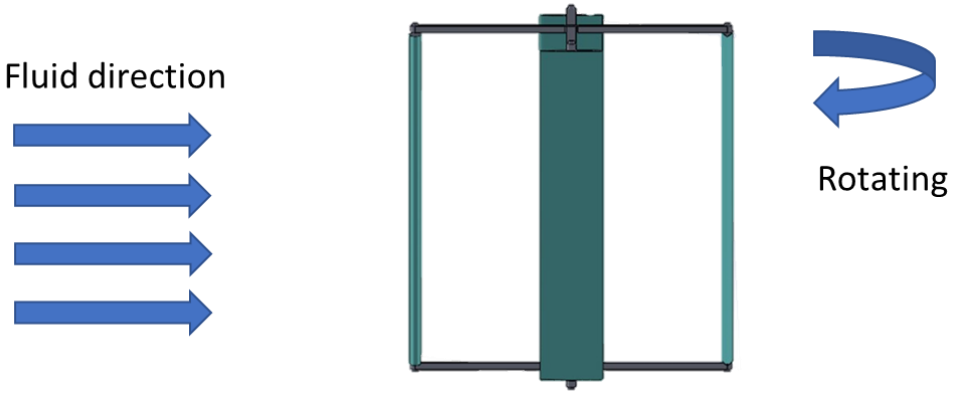

Figure 1. Working principle of H-Darrieus turbine

For the H-Darrieus turbine design, the most critical part that will contribute to the turbine's performance is the airfoil design. There are a few airfoil designs on deck, which are NACA 4-digit, S-series, A-series and FX-series. Usually, most of the blade designs will use NACA 4-digit series. There are two types of 4-Digit series, which are symmetrical and non-symmetrical designs as shown in Figure 2. The most common and less complex design will be the symmetrical 4-Digit series. Moreover, these NACA 4-digit series are very common for wind turbine construction [9].

Figure 2. Symmetrical and non-symmetrical airfoil design

Another parameter that can influence the performance of the H-Darrieus turbine is the length of the airfoils or the chord length. Increasing the length of the airfoil will improve the Reynolds number; however, this action will reduce the efficiency of the blade. Additionally, the solidity of the turbine will also increase, thus affecting the turbine's peak performance [10]. The solidity of the turbine is increased by increasing the chord length of the NACA blade and decreasing the number of blades of the H-Darrieus turbine [11]. Figure 3 shows the chord length diagram of the airfoil.

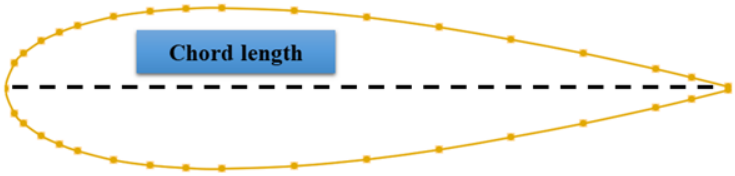

Figure 3. Chord length of the airfoil

Savonius Turbine

Savonius turbine is a vertical turbine that has a very simple design and uses the drag force from the fluid to rotate the device. The conventional design of the Savonius turbine consists of two half bucket blades mounted on the same axis to create an s-shape turbine design, as illustrated by Figure 4 [12].

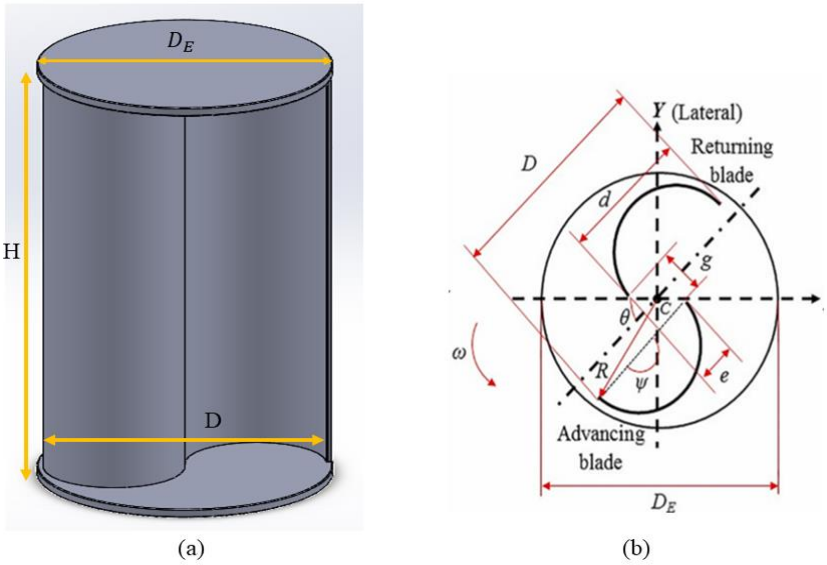

Figure 4. Conventional Savonius turbine with endplate design [12]

In order to increase this conventional Savonius turbine performance, there are a few parameters that can be modified and changed. The easiest modification that can be done is by increasing the gap ratio between the two blades. This modification helps the turbine to reduce the pressure acting on the head of the turbine. Besides that, it can also increase the torque performance of the turbine.

However, there are certain limits to the gap ratio. If the gap ratio is too much, the overall performance of the turbine will drop. This is because the fluid flow will change the direction of attack, which affects the returning blade of the turbine. Several studies had been conducted to identify the optimal gap ratio of the turbine [12]. The best range of the gap ratio between the blade is proposed to be between 0.2-0.25[6], but another study done by Yaakob Omar suggested that the Savonius turbine will have the best average torque at 0.1362Nm by using a gap ratio of 0.21 [6].

Other than that, adding endplates to the ends of the Savonius turbine also helps to increase the Savonius turbine's performance as shown in Figure 5. The purpose of the endplates is to overcome the problem of pressure difference and fluid leaking out. The endplates will maintain the constant drag force acting on the turbine, which helps in the performance of the turbine. Patel et al had experimented by adding endplates to the turbine and they reported significant improvements in the power coefficient of the turbine. Turbines with endplates demonstrated an overall improvement of about 80% compared to the turbine without endplates [13].

The starting performance of a conventional Savonius turbine is slower compared to other vertical turbines. In order to improve the starting performance of the turbine, the number of stages needs to be increased. By increasing the number of stages, the static torque will decrease; hence, the starting capability and performance of the turbine will also increase [14]. Figure 5 shows the double stages Savonius design with endplates.

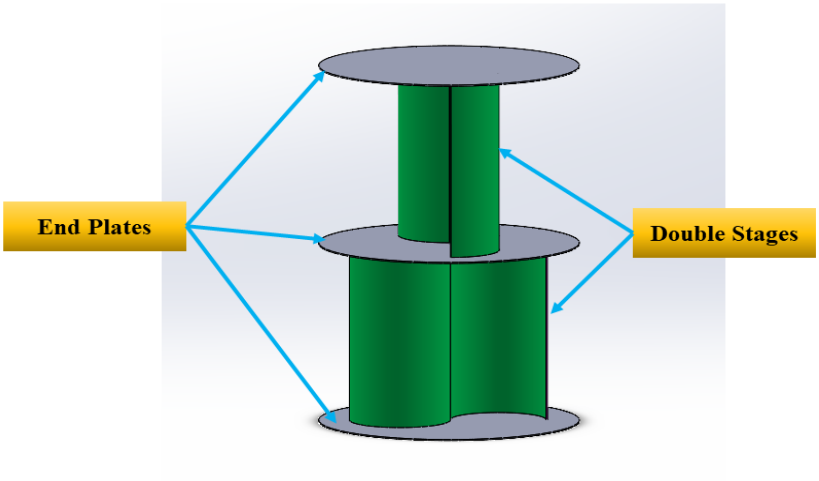

Figure 5. Double Stages Savonius with endplates

Hybrid Turbine

A hybrid turbine design is a combination of two turbines. In this case, Savonius and Darrieus turbines are used as a variety of hybrid turbines. Savonius is a drag base turbine and it has a high starting torque. The downside of the Savonius turbine is that it has low efficiency. As for the H-Darrieus turbine, it is a lift base turbine and it has high efficiency. However, the Darrieus turbine has a poor starting torque. Therefore, combining these two turbines, can help to solve each turbines' disadvantages. Moreover, it can also produce power at a lower flow speed. There are a few combinations that can be done by using these two turbines, such as, by mounting the Savonius turbine on top or below the H-Darrieus turbine. Another option is by mounting the Savonius turbine in the middle of the H-Darrieus turbine, which is called as a nested turbine. The arrangement of Savonius turbine on the top or below the H-Darrieus turbine can generate unwanted vibration due to the length of the device. In order to avoid this issue, these two devices can be combined in a nested form which able to reduce the unwanted vibration and also generate higher power coefficient at a low speed [15,16]. Figure 6 illustrates the hybrid nested turbine.

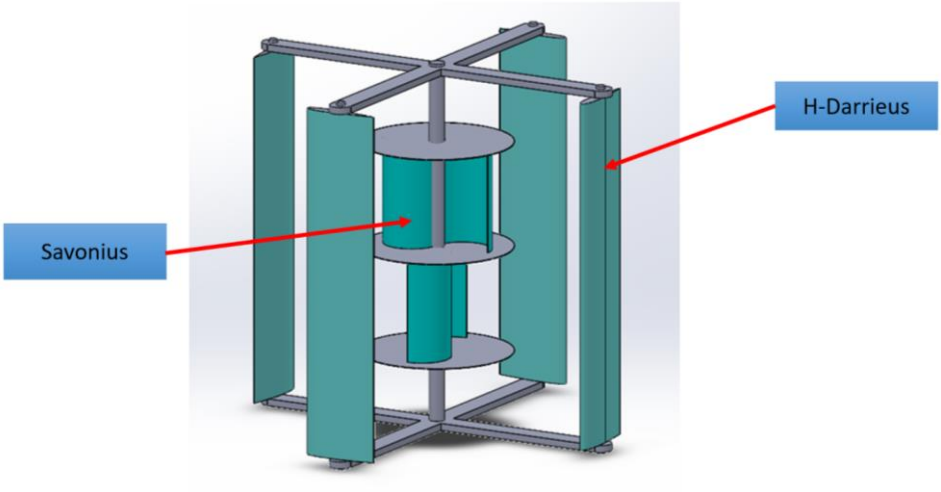

Figure 6. Hybrid turbine in nested form

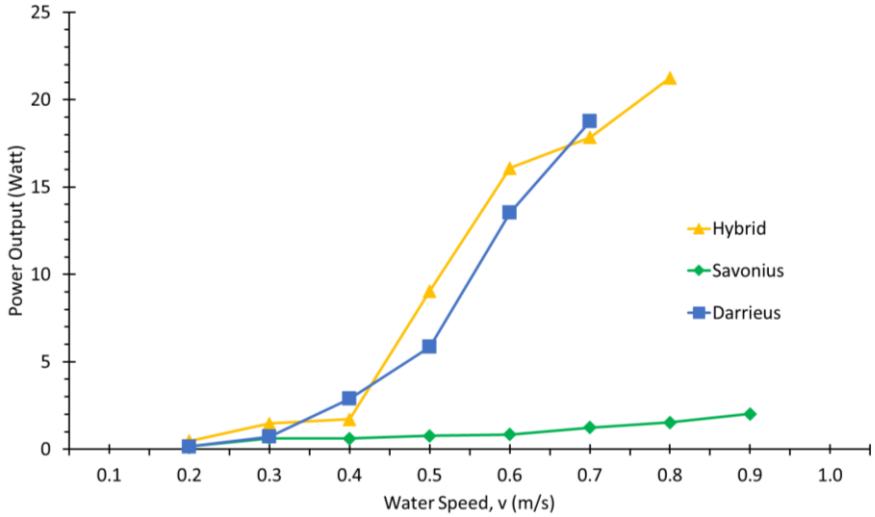

Figure 7. Comparison of the power output of three vertical turbines [17]

Figure 7 shows the graph of the power output produced by each vertical turbine from an experimental study. The hybrid turbine starts to generate power output at a slower speed than the Savonius and Darrieus turbines at 0.2m/s. The maximum power output for the hybrid turbine occurs at the speed of 0.8m/s at 21.3 watts. As for the Darrieus and Savonius turbines, the power starts to generate at 0.3m/s and the maximum power output for the Darrieus turbine is 19 watts at a maximum speed of 0.7m/s. Savonius turbine will achieve its peak performance at 1.0m/s with a power output of 2.13 watts. From the power output graph, the hybrid turbine peak performance range is from 0.6m/s to 0.8m/s. The hybrid turbine will not reach its peak performance at a higher speed due to its limitation of design [17].

Efflux Velocity Distribution Equation of Tidal Turbine

As illustrated by Figure 8, a turbine wake can be divided into two regions, which is near wake and far wake. Near wake is defined by the downstream position 1D behind the turbine, where D refers to the device diameter. Far wake, meanwhile, is defined as a location further away across the downstream of the turbine. The formation of the wake is due to the velocity difference or the transfer of kinetic energy from high-velocity flow to low-velocity flow, which is known as turbulent mixing. The term efflux velocity can be defined as minimum velocity from the average time and downstream domains: the efflux velocity can help to determine the velocity deficits at the downstream region [18].

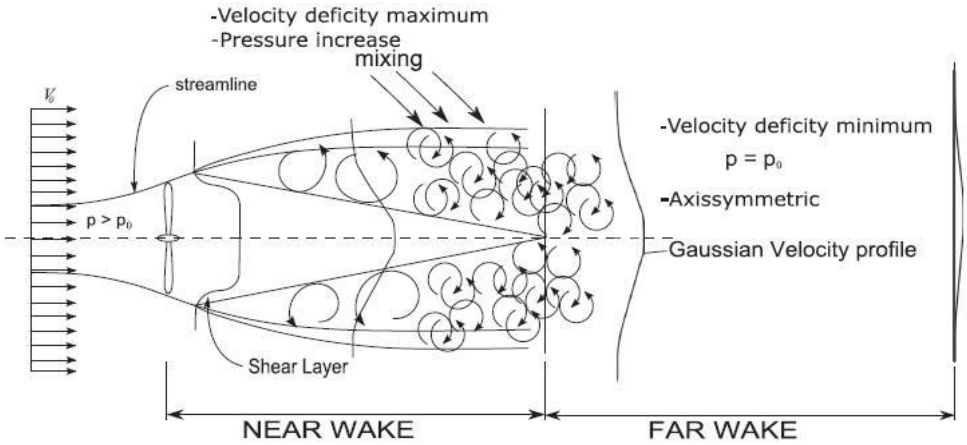

Figure 8. Turbulent mixing downstream [19]

Derivation of Velocity Equation of Tidal Turbine Wake

The wake properties can be solved by taking Eq. (1) which is the Gaussian probability distribution equation into consideration and applying it to the velocity deficit downstream of the device as proposed [18]. From Eq. (1), $V_{x,r}$ is the lateral direction of the velocity, V_{max} is the maximum lateral distribution velocity in m/s, D_{or} is the diameter of the orifice,V_{∞} is the free stream velocity in m/s and σ is the standard deviation of the velocity for the lateral plane. Then, by substituting Cx (constant velocity in x direction) for σ and changing r (radial distance), Eq. (1) is then evolved into Eq. (2) [18].

$$\frac{V_{x,r}}{V_{max}} = e^{\left[-\left(\frac{r^2}{2\sigma^2}\right)\right]} \quad (1)$$

$$\frac{V_{x,r}}{V_{max}} = e^{-\left(\frac{\left(r+Cx-\left(\frac{D_{or}}{2}\right)\right)^2}{2(Cx)^2}\right)} \tag{2}$$

$$V_{x,r} = V_{\infty}\{1 - e^{\left[-\left(\frac{r^2}{2\sigma^2}\right)\right]}\} \tag{3}$$

$$V_{x,r} = V_{\infty} - \{V_{\infty} - V_{\min}\}e^{[-\left(\frac{r^2}{2\sigma^2}\right)]} \tag{4}$$

By changing the exponential to negative terms, Eq. (3) is achived. Thus, V_{min} is taken into consideration by adding it into the formula to get Eq. (4).

$$V_{x,r} = V_{\infty} - \{V_{\infty} - V_{\min}\}e^{[-(\frac{\left(r+Cx-\left(\frac{D_t}{2}\right)\right)^2}{2(Cx)^2})]} \tag{5}$$

$$V_{x,r} = V_{\infty} - \{V_{\infty} - V_{\min}\}e^{[-(\frac{\left(r+0.081x-\left(\frac{D_t}{2}\right)\right)^2}{2(0.081x)^2})]} \tag{6}$$

Next, by substituting Cx for σ then replacing r with the potential terms, the final velocity distribution is achieved as shown in Eq. (5). Taking D_t as the turbine diameter, assuming x/D_t = 6.2 and by substituting C (lateral velocity distribution constant) as 0.08, that will give us Eq. (6). This derivation of tidal wake characteristics is similar to the one proposed for a propeller jet [18].

Steady-State Reynolds-Average Navier-Stokes Equation (RANS)

RANS model is an equation that computes the average flow of fluid in an incompressible manner. The simulation that uses RANS will have faster simulation time compared to Large Eddy Simulation (LES). However, the downside of RANS is that it cannot compute flow in more accurate manner such as LES. Additionally, LES can detect variation of unsteady flow and capture more detail results in the near wake condition. The limitation of LES is the requirement of computation power and the time taken for the simulation process[20, 21]. Equation (7) displays the steady-state RANS formulation;

$$\frac{\partial}{\partial x_j}\left(\overline{\rho u_i u_j}\right) = -\frac{\partial \bar{p}}{\partial x_i} + \frac{\partial}{\partial x_j}\left[\mu\left(\frac{\partial \overline{u_i}}{\partial x_j} + \frac{\partial \overline{u_j}}{\partial x_i} - \frac{2}{3}\delta_{ij}\frac{\partial \overline{u_l}}{\partial x_l}\right)\right] + \frac{\partial}{\partial x_j}\left(-\overline{\rho u_i' u_j'}\right) \tag{7}$$

Where the,$\bar{u}$ is the velocity in time average, $\bar{p}$ is the average pressure, $\bar{\rho}$ is the average fluid density, μ is the fluid viscosity and $-\overline{\rho u_i' u_j'}$ is the Reynolds stress.

Standard k-epsilon Model

A standard k-epsilon model is typically used for turbulent modeling in any flow simulation. It is a powerful and robust equation that can be used in a vast range of engineering problem. The equation can also produce accurate simulation results with less computational power [21]. The transportation equation for k and ε are derived as follows:

$$\frac{\partial}{\partial x_i}(\rho k \overline{u_i}) = \frac{\partial}{\partial x_j}\left[\left(\mu + \frac{\mu_t}{\sigma_k}\right)\frac{\partial \varepsilon}{\partial x_j}\right] + G_k - Y_k \tag{8}$$

$$\frac{\partial}{\partial x_i}(\rho \varepsilon \overline{u_i}) = \frac{\partial}{\partial x_j}\left[\left(\mu + \frac{\mu_t}{\sigma_\varepsilon}\right)\frac{\partial \varepsilon}{\partial x_j}\right] + G_\varepsilon - Y_\varepsilon \tag{9}$$

Where k is the turbulent kinetic and ε turbulent dissipation, μ_t is the eddy viscosity. Equations (8) and (9) show the turbulent Prandtl number which is the σ_k and σ_ε. Next is the turbulent kinetic energy equation that is compatible with Boussinesq hypothesis;

$$G_k = \mu_t S^2 \tag{10}$$

S in the equation is defined by the average rate-of-strain tensor;

$$S = \sqrt{2S_{ij}S_{ij}} \tag{11}$$

$$S_{ij} = \frac{1}{2}\left(\frac{\partial \overline{u_j}}{\partial x_i} + \frac{\partial \overline{u_\iota}}{\partial x_j}\right) \tag{12}$$

Y_k is the dissipation of kinetic energy generated by the turbulence flow;

$$Y_k = \rho\varepsilon \tag{13}$$

Then dissipation of $G_\varepsilon, \varepsilon$ and Y_ε are explained as:

$$G_\varepsilon = C_{1\varepsilon}\frac{\varepsilon}{k}(G_k) \tag{14}$$
$$Y_\varepsilon = C_{2\varepsilon}\rho\frac{\varepsilon^2}{k}$$

The turbulent viscosity is computed from the k and ε with a constant value of $C_{1\varepsilon}$ and $C_{2\varepsilon}$;

$$\mu_t = \rho C_\mu \frac{k^2}{\varepsilon} \tag{15}$$

From Eq. (15) and considering C_μ is constant, then, the remaining variables used for the standard k-epsilon models equation are summarised as in Table 1 [21]:

Table 1. Constant variable for k-epsilon models

Constant	Value
$C_{1\varepsilon}$	1.44
$C_{2\varepsilon}$	1.92
C_μ	0.09
σ_k	1.0
σ_ε	1.3

METHODOLOGY

The initial step of this research is to gather information about types of tidal turbines, specifically on vertical tidal turbine design. A hybrid nested turbine requires a few geometrical parameters to be set, as this turbine design involves two vertical turbines, namely Savonius and H-Darrieus. The first parameter to be studied is the NACA blade design on the nested hybrid turbine. The turbine CAD models were designed and drawn by using SolidWorks, while the numerical simulation used was Ansys CFD Fluent [22]. The simulation data was then transferred to Matlab for post-processing step. Then, the results were validated with published data from a study conducted by Harrison et al. [27]. Figure 9 shows the reasearch flow chart for this study.

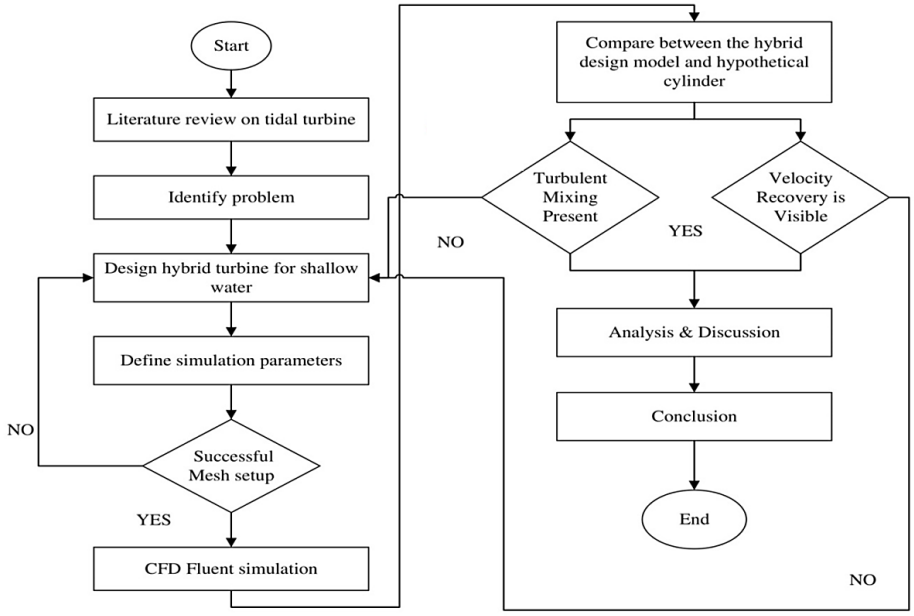

Figure 9. Research work flow for this study

Design of H-Darrieus Turbine

Three airfoil designs were used for the simulation, which are NACA0015, NACA0018 and NACA0021 symmetric geometry as shown in Figure 10. These airfoil designs come under the 4-digit NACA series category. These series are commonly used in wind turbine operations. Their manufacturability is also more simple compared to other NACA blade series. The turbine design will have different thicknesses in terms of blade geometry. Although a thicker blade will produce more drag force, it also will help to increase the lift force on the turbine. Table 2 displays the design parameters used for H-Darrieus turbine in this study.

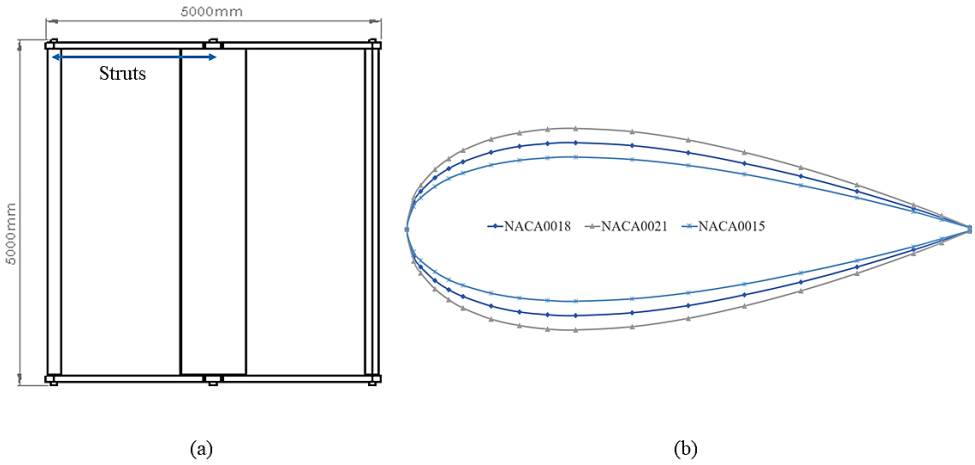

Figure 10. (a) H-Darrieus turbine design and (b) NACA blade design

Table 2. H-Darrieus design parameters

Parameters	Details/values
Type of blade	NACA0015, NACA0018, NACA0021
Number of blades	4
Chord length	1000mm
Height	5000mm
Diameter	5000mm
Struts length	2449.49mm
Height and diameter ratio Ø	1

Design of Savonius Turbine

Since the conventional design of the Savonius turbine is not efficient for power extraction, few modifications can be done to the Savonius turbine in order to increase the performance. One modification done was by adding endplates to the turbine to increase the rotating power in producing more mechanical torque. Additionally, the number of stages was increased by one to help the turbine improve its self-starting capability. Figure 11 and Table 3 illustrate the geometrical design and parameters used for the Savonius turbine in this study.

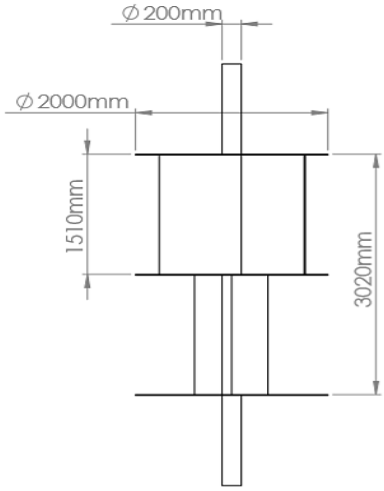

Figure 11. Double stage Savonius turbine

Table 3. Savonius design parameters

Parameters	Details/values
Turbine height	3020mm
Turbine diameter	2000mm
Shaft diameter	200mm
Nominal diameter of blade	1507.5mm
Radius of each blade	376.88mm
Number of blades	2
Number of stages	2
Overlap ratio	0.2
Endplate ratio	1.2
Aspect ratio	2.0
Phase shift	90˚

Hybrid Nested Turbine

Figure 12 shows the combination of hybrid turbine (Savonius and H-Darrieus) using the nested combination. Based on previous studies, this combination of hybrid turbine should be able to reduce the vibration and also increase the power coefficient. However, the downside of this combination is that it produces less electricity [23].

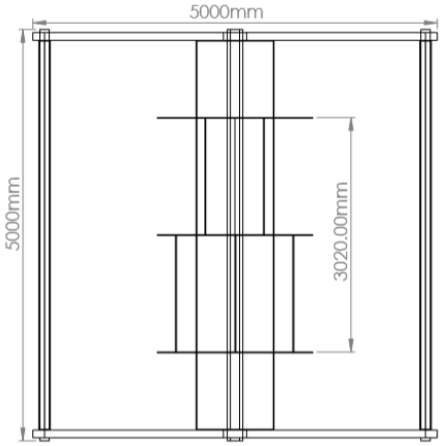

Figure 12. Hybrid turbine in nested combination

CFD Domain Dimension

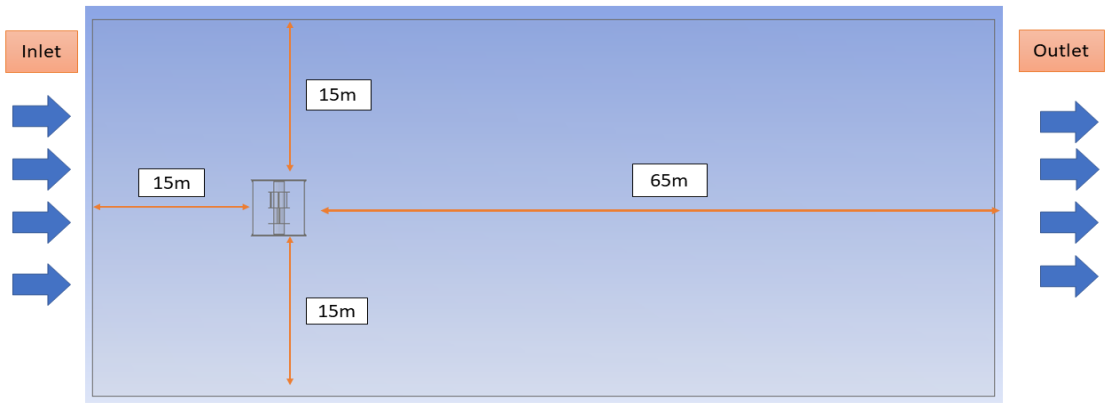

Figure 13. Domain dimension of CFD simulation (Side View)

Figure 13 shows the domain size used for the CFD Fluent simulation in Ansys. As displayed in Figure 13, the gap used for the top and bottom of the turbine is about 15m, and the downstream domain is about 65m [24]. Since this study focuses on the turbulent mixing and the velocity deficits of the turbine design, the downstream domain needs to be longer, which is set at 65m to investigate the turbulent mixing.

Meshing Configurations

Figure 14 (a) shows the meshing result of the outer boundary wall of the turbine and Figure 14 (b) displays the turbine meshing which is located in the inner domain walls. The size of the meshing used was set to fine, where the average domain elements were roughly about 1.4m. More importantly, the minimum element size was about 0.015m, which is predominantly located near the turbine. Setting the mesh size to fine should be able to generate a result that is more accurate and stable. When the meshing size is fine, the computed variables can travel from one node to another node quickly and more accurately. The generated mesh employed tetra elements that are suitable for complicated design. The hybrid turbine model consists of complex geometries such as the NACA blade design and double stage Savonius turbine. The meshing was done by using the default setting in ANSYS which helped to generate the most compatible element size for the domain and turbine. The meshing generated was good enough to run the simulation with low skewness values [25]. Additionally, the element size cannot be set to be smaller than the current setting due to constraints in computational resources.

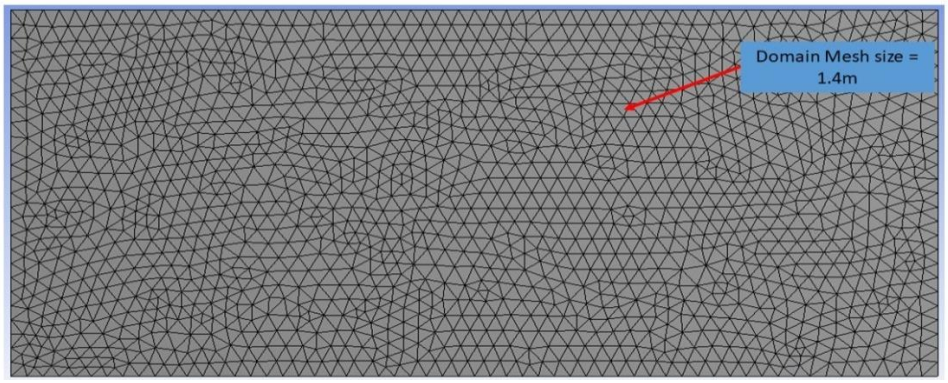

(a)

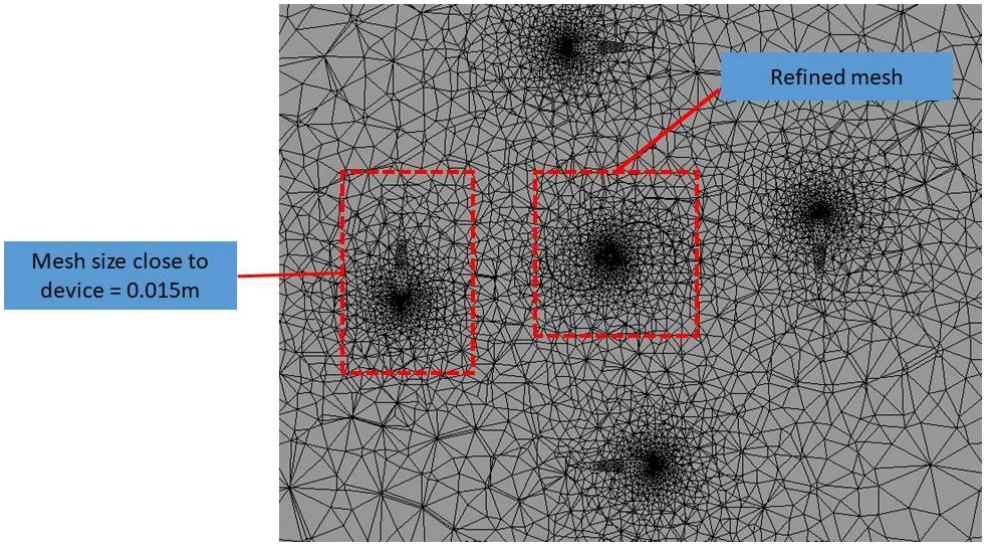

(b)

Figure 14. (a) Domain meshing (enclosure of the turbine) and (b) Hybrid nested turbine meshing

Study Parameters

Table 4 displays the parameters that are imposed in the simulation process based on the literature. The viscosity and seawater density is taken from the average water temperature value at 27 ℃ [26]. The lower velocity value is based on Yaakob Omar's study, where the average velocity of Malaysia's open water was stated to be at 0.6m/s [6] while the higher speed current velocity was gathered from A. Bakri [24]. Next, the k-epsilon model was employed because of its robustness, requires less computational power and the equation generated by the model is usually used for the initial simulation study. The second-order equation, known as a linear equation that can capture more physical data compared to the first-order equation, was chosen for its accuracy and computational time.

Table 4. Parameters for simulation setup

Parameters	Details/values
Viscosity	0.00092 Ns/m^2
Velocity	0.6m/s & 1.0 m/s
Seawater density	1023 kg/m^3
Turbulence Models	k-epsilon
Equation	Second-order

Extraction of Velocity Results

Figure 15 demonstrates the positioning of the slicing performed on the domain for data extraction. The data was extracted at 5D, 7D and 9D positions downstream of the device [27]. The 'D' on slicing refers to the diameter of the turbine. For instance, the 5D represents 5 multiplied by the diameter of the turbine (which is 5 meters) which gives us a distance of 25 meters behind the device. Table 5 shows the extraction distance to be used for plotting the wake velocity recovery based on the lateral position of the domain.

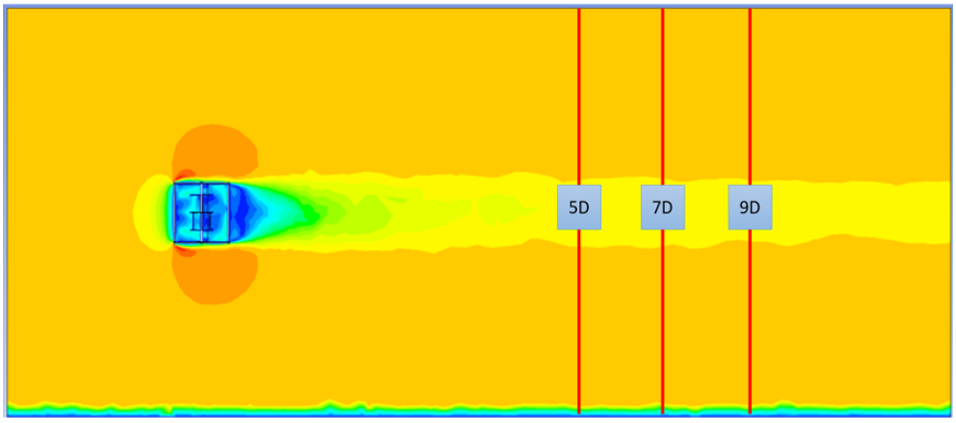

Figure 15. Location of slicing for data extraction in the domain

Table 5. Slicing position for plotting wake recovery velocity

Slicing	Distance
5D	25 meter
7D	35 meter
9D	45 meter

SIMULATION RESULTS

Two comparison studies are presented and discussed in this section which is the influence of different current velocities used (i.e. 0.6m/s and 1.0m/s) and also a comparison between hypothetical actuator cylinder and three hybrid nested turbines that employ NACA0015, NACA0018 and NACA0021 respectively. All CAD models are set to have the same diameter and height, which is 5 meters for both height and diameter as illustrated in Figure 16.

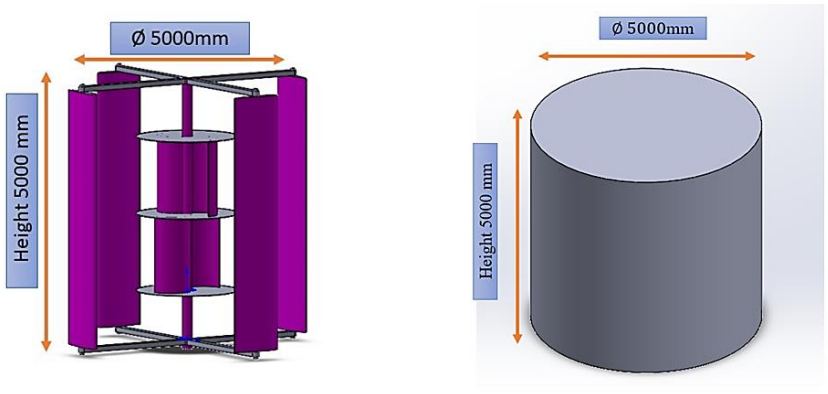

(a) (b)

Figure 16. (a) Hybrid nested turbine (b) Hypothetical actuator cylinder [24]

Wake Turbulence for 0.6m/s

Figure 17,18,19 and 20 demonstrate the turbulent mix of a hybrid nested turbine with different NACA blade designs and hypothetical actuator cylinder. For the hybrid nested turbine, NACA0021 generates a bigger deceleration of flow at the upstream region followed by hybrid nested NACA0015 and NACA0018. On the other hand, a hypothetical actuator cylinder shows a smaller deceleration at the upstream region than a hybrid nested NACA0021 turbine.

For the downstream region, where the turbulent mixing will occur, hybrid nested using NACA0015 and 0018 display a more narrow turbulent mix compared to hybrid nested NACA0021. This shows that the kinetic energy from the high-velocity flow is transferred faster to the low kinetic energy for the low velocity for the hybrid nested NACA0015 and 0018. Hence, the acceleration of the momentum for hybrid nested NACA0021 is slower than hybrid nested NACA0015 and 0018. The reason for this occurrence is due to the blade design of NACA. NACA0015 has better aerodynamic efficiency and NACA00018 has a better starting capability than NACA0021 [28]. As for the cylinder, the turbulent mix at the downstream region is not as accurate as in the turbine models, but it still shows a small amount of mixing.

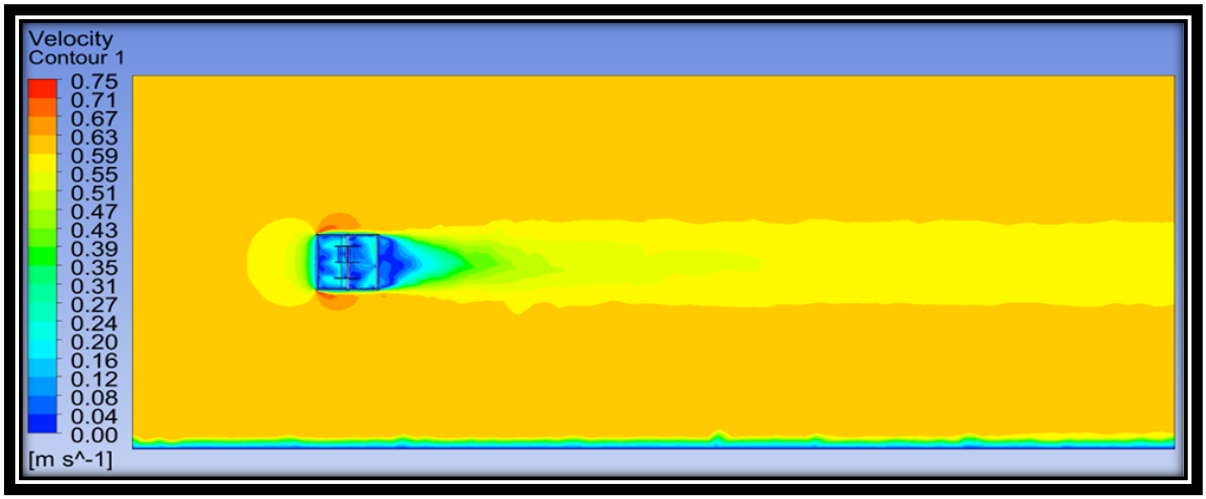

Figure 17. Hybrid nested NACA0015 at 0.6m/s velocity

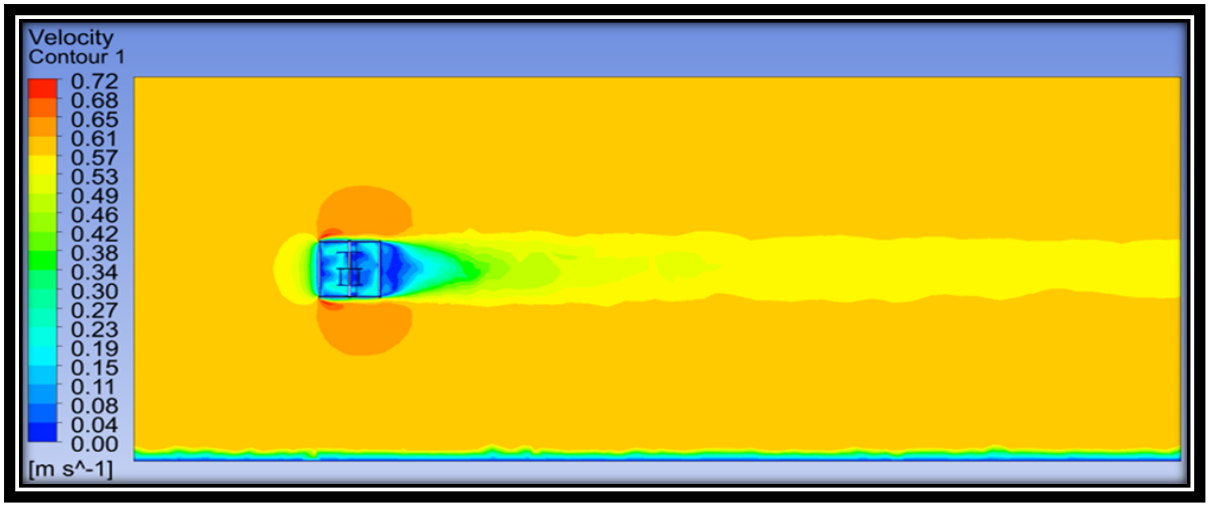

Figure 18. Hybrid nested NACA0018 at 0.6m/s velocity

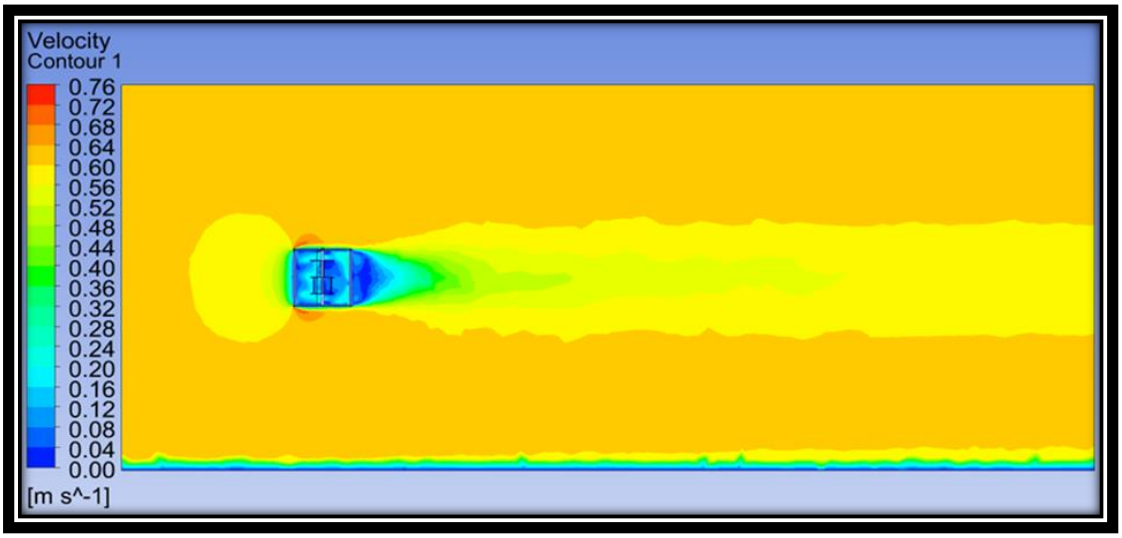

Figure 19. Hybrid nested NACA0021at 0.6m/s velocity

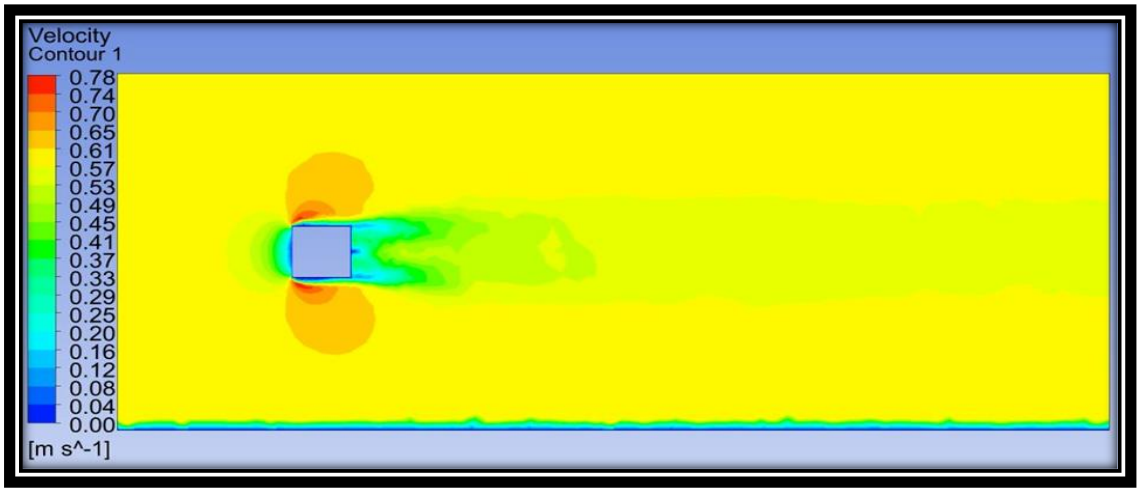

Figure 20. Hypothetical cylinder at 0.6m/s velocity

Wake Turbulence for 1.0m/s

Figure 21, 22, 23 and 24 show the results for 1.0m/s velocity, the turbulent mixing outcome for the hybrid nested turbine is almost similar to the one presented for 0.6m/s. The result for the velocity contour did not show any significant change because of the limitation of the simulation used since RANS can only compute the averaged result and cannot show the detailed result of the near wake region close to the turbine. Vortex shedding phenomena does occur in the simulation as illustrated by the velocity deficits shown in the contour plots. However, due to the limitations of RANS simulation, the resulting vortex shedding characteristics are not obvious enough to be observed. As noticed from all of the velocity contour plots for 0.6m/s and 1.0m/s, hybrid nested NACA0018 shows a huge energy release, represented by the red contour plot. Then, the nested NACA0018 result also shows a small gap at the downstream region where the turbulent mix occurs which can be observed in Figure 18 and Figure 22. The small gap indicates vorticity formation due to the blade thickness design of the NACA blade. Hence, it is evident that vorticity can impact the overall performance of the turbine in terms of velocity recovery and also power generation [29, 30].

In a conclusion, from the results presented, the thickness of airfoils blades plays an important role in the nested turbine performance in regards to velocity recovery.

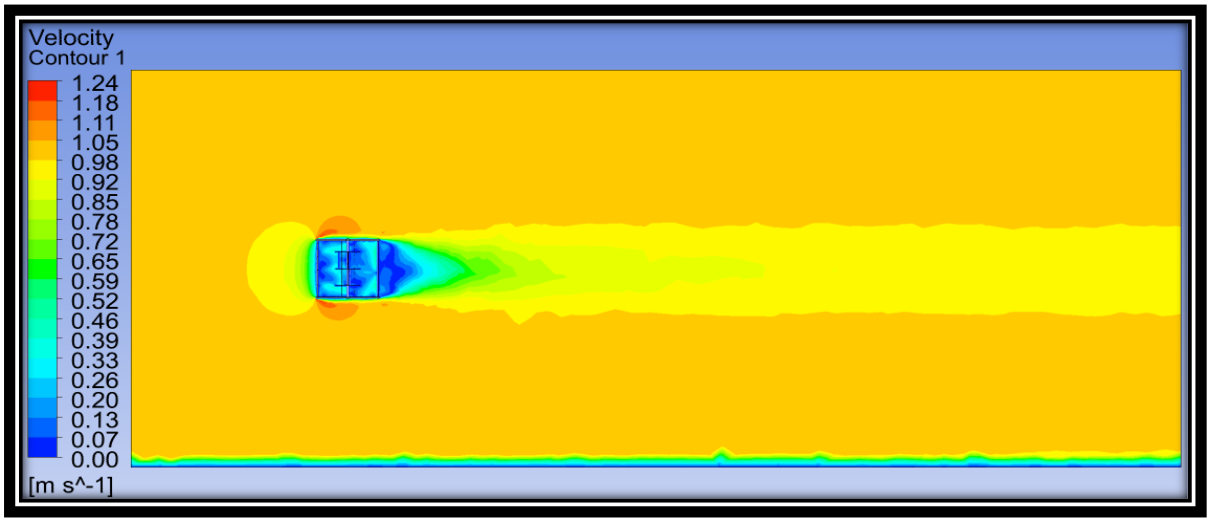

Figure 21. Hybrid nested turbine NACA0015 at 1.0m/s velocity

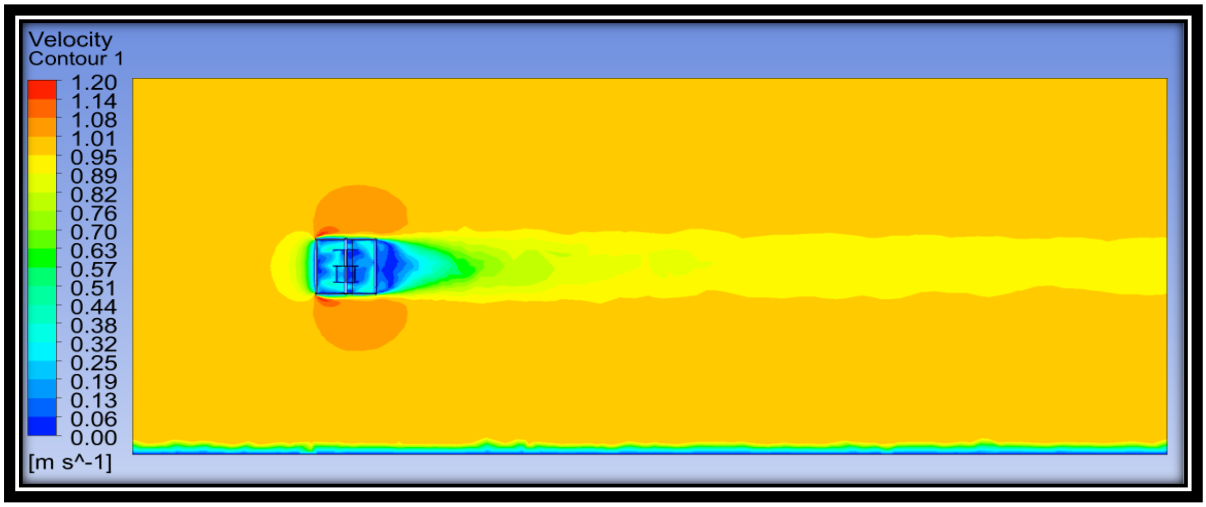

Figure 22. Hybrid nested turbine NACA0018 at 1.0m/s velocity

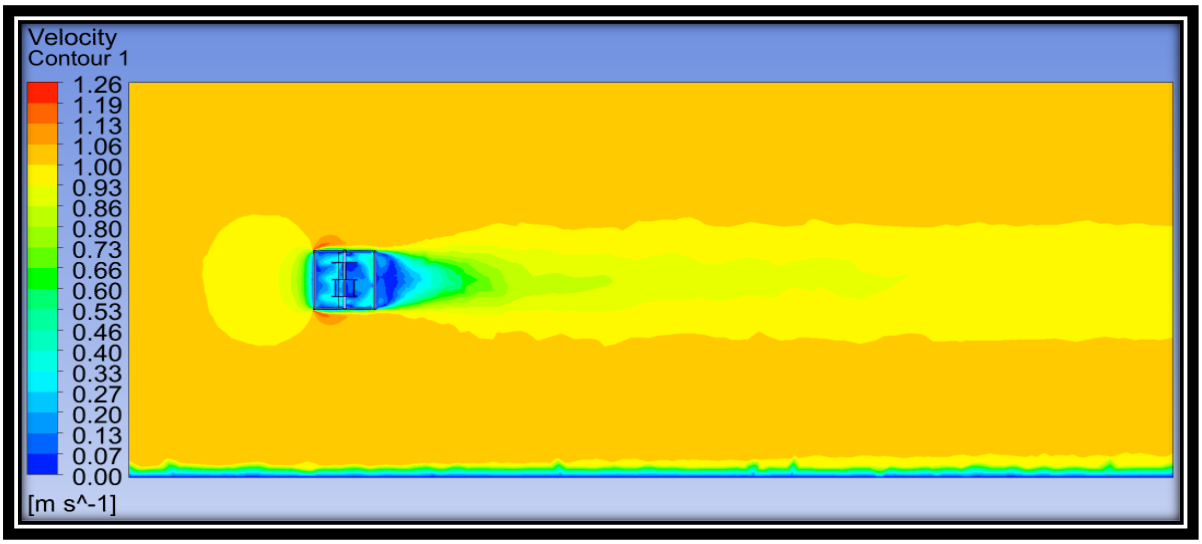

Figure 23. Hybrid nested turbine NACA0021 at 1.0m/s velocity

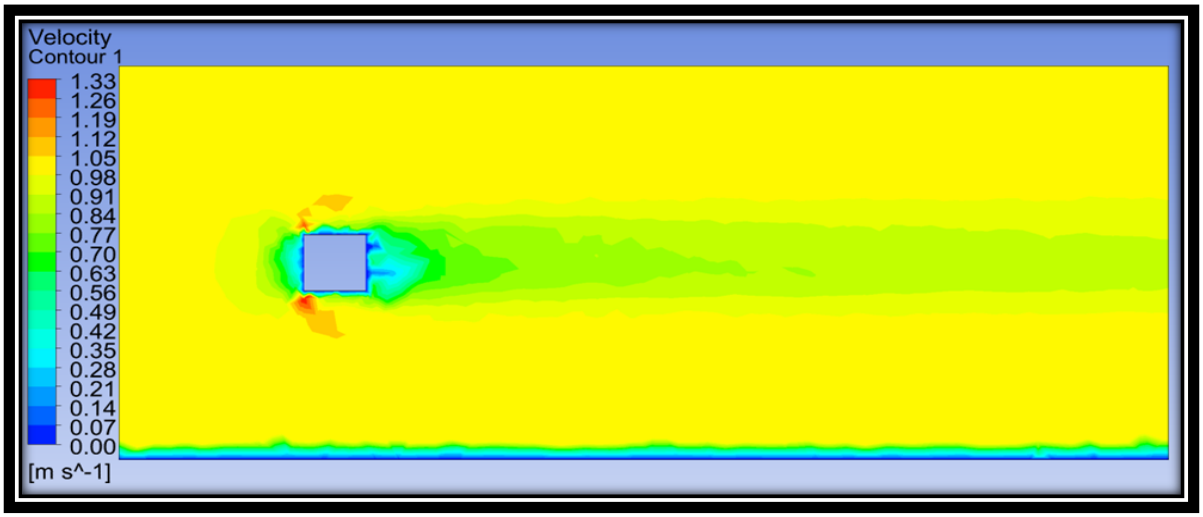

Figure 24. Hypothetical cylinder at 1.0m/s velocity

Validation between the hybrid nested turbine and hypothetical actuator cylinder in terms of velocity recovery

Velocity 0.6m/s

Figure 25 shows the downstream recovery of the flow for 0.6m/s. From the graph, markers 'o' represents the data of the hypothetical cylinder study done by Bakri.A [24]. All the hybrid nested turbine results are compared with the cylinder. From the 5D graph, the hybrid nested NACA0018 exhibits the highest deficits followed by NACA0015. Moving on to the 7D plot, the NACA0018 flow starts to recover faster, while the hybrid nested NACA0015 demonstrates the highest velocity deficits at this point. On the 9D position, nested NACA0015 shows faster flow recovery when compared to NACA0018. As for the hypothetical cylinder and hybrid nested NACA0021, both models do not show any significant velocity recovery. This is due to the design of the blade for NACA0021 which has a thicker blade design that can impact the flow recovery. These plots also help to explain the turbulent mixing result as the acceleration flow for the hybrid nested NACA0015 and NACA0018 are faster than hybrid nested NACA0021.As for the $\frac{U}{U_0}$ Figure 25 and Figure 26 is not equal to 0.6m/s and 1.0m/s at 9D is because the velocity flow has not been fully recovered.

A hypothetical actuator cylinder representing the standalone VATT turbine demonstrates similar trends according to the graph. The actuator cylinder's results were then compared to the output from the real turbine models in terms of the percentage deviation as shown in Table 6. Based on the table, it can be seen that the percentage deviation does not exceed 10%, which agrees well with Bakri. A's study [24].

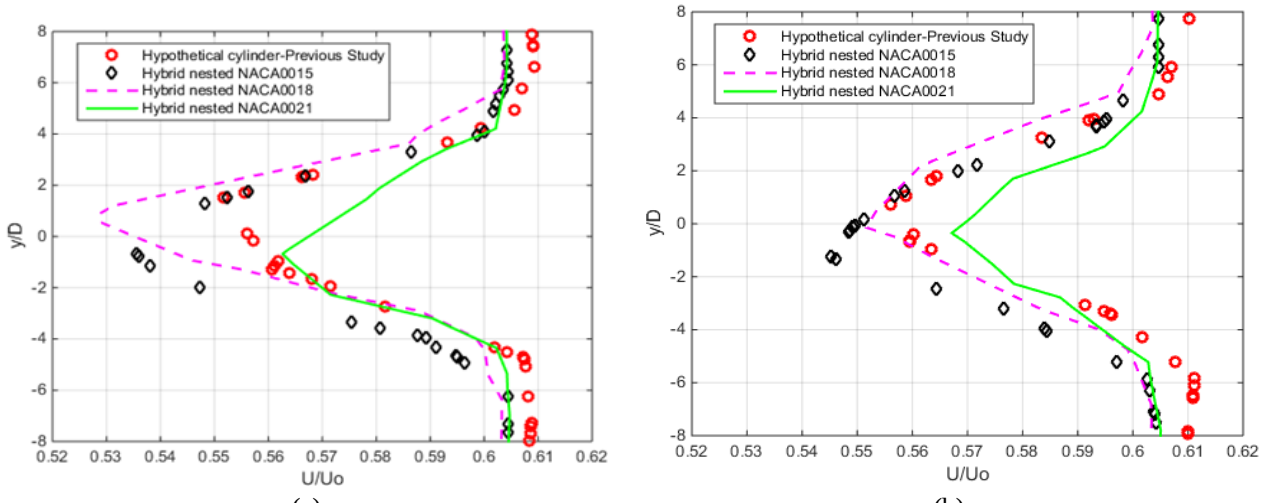

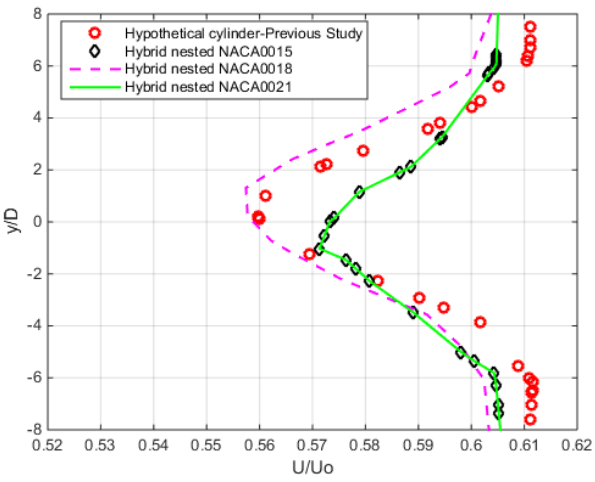

$U_0 = 0.6m/s$

(c)

Figure 25. Velocity recovery at (a) 5D (b) 7D (c) 9D for 0.6m/s

Table 6. Percentage deviation for 0.6m/s

Hybrid nested turbine	NACA0015	NACA0018	NACA0021
Deviation (5D)	2.85%	4.14%	1.93%
Deviation (7D)	1.94%	0.78%	1.96%
Deviation (9D)	1.99%	0.39%	2.04%

Velocity 1.0m/s

For the 1.0m/s speed, the flow recovery for the hypothetical cylinder shows the biggest velocity deficits at all positions as illustrated in Figure 26. For the hybrid nested turbine, NACA0018 shows a similar characteristic with the 0.6m/s results for 5D and 7D. As for the 5D, it has the biggest deficits among the hybrid nested turbines. 7D NACA0018 turbine meanwhile shows faster recovery compared to NACA0015. Next, the 9D plot shows a different outcome compared to the slower 0.6m/s velocity where at 1.0m/s, the hybrid nested NACA0018 has a faster velocity recovery than hybrid nested NACA0015. However, the turbulent mixing for the 1.0m/s velocity did not show a high mixing rate compared to the 0.6m/s flow, which can be observed from the velocity recovery graph from the 5D, 7D and 9D graphs (Figure 25 and Figure 26). The 0.6m/s flow shows a faster recovery compared to the 1.0m/s. This could be explained by the fact that the drag force produced by the Savonius turbine is higher at 1.0m/s compared with 0.6m/s. The results also proved that a hybrid nested turbine works optimally at a low-speed current.

From all the simulation result graphs, it can be distinguished that nested NACA0015 and NACA0018 exhibit a faster velocity recovery from the 5D to the 9D position compared to nested NACA0021. These observations can be clearly examined in Figure 25. Although the hypothetical cylinder did show a decent amount of velocity recovery, the results are not as accurate as an actual standalone (VATT) design. Based on Table 7, the velocity output between the three designs are still comparable as the percentage deviation for each of the hybrid nested turbines against the hypothetical actuator cylinder is still under 10%.

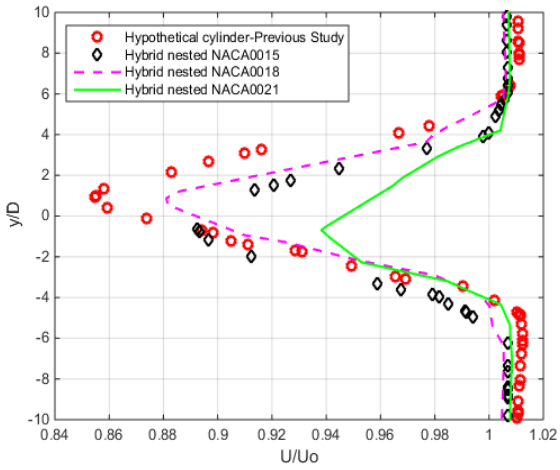

(a)

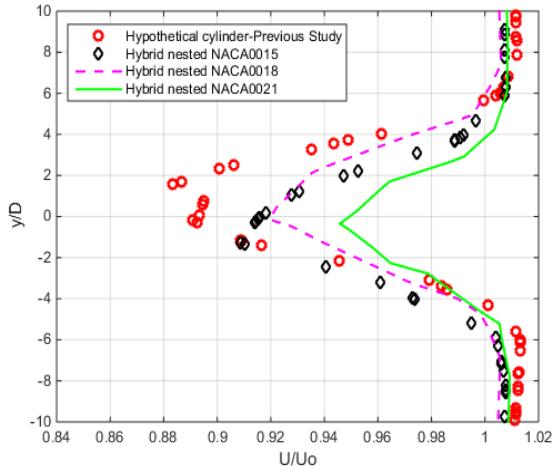

(b)

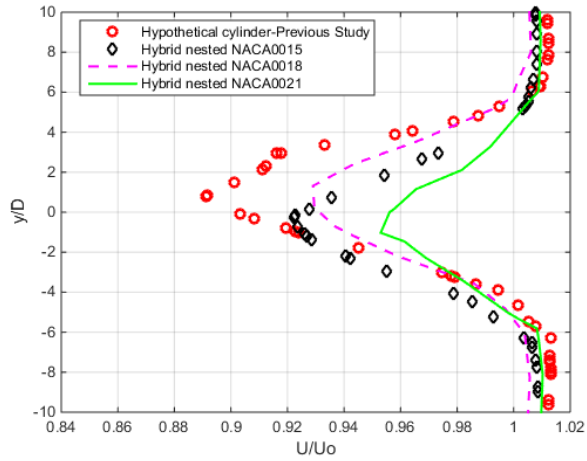

$U_0 = 1.0m/s$

(c)

Figure 26. Velocity recovery at (a) 5D (b) 7D (c) 9D for 1.0m/s

Table 7. Percentage deviation for 1.0m/s

Hybrid nested turbine	NACA0015	NACA0018	NACA0021
Deviation (5D)	4.28%	3.00%	8.8%
Deviation (7D)	2.80%	3.94%	3.94%
Deviation (9D)	3.46%	4.10%	6.63%

CONCLUSION

From the numerical simulation conducted, the optimal design for a hybrid nested turbine for shallow water application has been identified, which is hybrid nested NACA0015 and 0018. Both of these turbines show great velocity recovery at the downstream region. Additionally, for the NACA0015 blade, it offers a better recovery towards the 9D area for the 0.6m/s velocity. However, when the flow velocity increases to 1.0m/s, the hybrid nested turbine did not perform well for the wake to recover to its ambience velocity. As Savonius turbine produces a bigger drag force which affects the flow recovery, the hybrid nested turbine with NACA0015 and 0018 performed best when the flow speed is between 0.6m/s to 0.8m/s. The result of this simulation accomplishes the first objective of this study.

The second objective was to compare the turbulent wake and velocity recovery between the hybrid nested turbine and a hypothetical actuator cylinder. From the results presented, the cylinder did not show any remarkable improvement in terms of velocity recovery. Nonetheless, the trends of the velocity recovery graph are similar with all the hybrid nested turbines models. Furthermore, the percentage velocity deviation of both 0.6m/s and 1.0m/s velocity is less than 10% which proves that the cylinder model is the ideal representation of a VATT turbine. Even though the results generated from the cylinder model were not as accurate as those of the real model design, they still provide useful data that can be used to understand general wake mixing characteristics.

ACKNOWLEDGEMENT

The authors gratefully acknowledge the financial support received from the Ministry of Higher Education Malaysia through the Fundamental Research Grant Scheme for Research Acculturation of Early Career Researchers (FRGS-RACER) - RACER/1/2019/TK07/UNIMAP/1.

REFERENCES

[1] Z. Liu, "Global energy development: The reality and challenges," *Glob. Energy Interconnect.*, vol. x, pp. 1–64, 2015, doi: 10.1016/b978-0-12-804405-6.00001-4.

[2] Energy Data and Research Unit, "Handbook Malaysia Energy Statistics," Suruhanjaya Tenaga (Energy Commission), ISSN No.: 2289-6953, 2019.

[3] N. A. Mohd Yusoff, N. L. Ramli, and M. R. Mohamed, "Investigation of the potential harnessing tidal energy in Malaysia," *ARPN J. Eng. Appl. Sci.*, vol. 10, no. 21, pp. 9835–9841, 2015.

[4] D. Satrio, I. K. A. P. Utama, and Mukhtasor, "Vertical axis tidal current turbine: Advantages and challenges review," *Proceeding Ocean. Mech. Aerosp. -Science Eng.*, vol. 3, no. July, pp. 64–71, 2016.

[5] D. Magagna and A. Uihlein, "Ocean energy development in Europe: Current status and future perspectives," *Int. J. Mar. Energy*, vol. 11, pp. 84–104, 2015, doi: 10.1016/j.ijome.2015.05.001.

[6] O. Bin Yaakob, K. B. Tawi, and D. T. S. Sunanto, "Computer simulation studies on the effect overlap ratio for savonius type vertical axis marine current turbine," *Int. J. Eng. Trans. A Basics*, vol. 23, no. 1, pp. 79–88, 2010.

[7] W. Tjiu, T. Marnoto, S. Mat, M. H. Ruslan, and K. Sopian, "Darrieus vertical axis wind turbine for power generation I: Assessment of Darrieus VAWT configurations," *Renew. Energy*, vol. 75, pp. 50–67, 2015, doi: 10.1016/j.renene.2014.09.038.

[8] A. S. Siddiqui et. al., "A review study : Distinct recent advancements in H-type Darrieus wind turbine to improve aerodynamic performance," *Proceedings of the International Conference on Renewable, Applied and New Energy Technologies*, 19–22 Nov., 2018.

[9] M. H. Mohamed, "Performance investigation of H-rotor Darrieus turbine with new airfoil shapes," *Energy*, vol. 47, no. 1, pp. 522–530, 2012, doi: 10.1016/j.energy.2012.08.044.

[10] A. Bianchini, G. Ferrara, and L. Ferrari, "Design guidelines for H-Darrieus wind turbines: Optimization of the annual energy yield," *Energy Convers. Manag.*, vol. 89, pp. 690–707, 2015, doi: 10.1016/j.enconman.2014.10.038.

[11] S. M. R. Hassan, M. Ali, and M. Q. Islam, "The effect of solidity on the performance of H-rotor Darrieus turbine," *AIP Conf. Proc.*, vol. 1754, 2016, doi: 10.1063/1.4958372.

[12] M. Badrul Salleh, N. M. Kamaruddin, and Z. Mohamed-Kassim, "Savonius hydrokinetic turbines for a sustainable river-based energy extraction: A review of the technology and potential applications in Malaysia," *Sustain. Energy Technol. Assessments*, vol. 36, no. September, p. 100554, 2019, doi: 10.1016/j.seta.2019.100554.

[13] V. Patel, T. I. Eldho. and S. V. Prabhu, G. Bhat, "Influence of overlap ratio and aspect ratio on the performance of Savonius hydrokinetic turbine," *Arch. Thermodyn.*, vol. 33, no. 4, pp. 23–40, 2012, doi: 10.1002/er.

[14] A. Kumar, R. P. Saini, G. Saini, and G. Dwivedi, "Effect of number of stages on the performance characteristics of modified Savonius hydrokinetic turbine," *Ocean Eng.*, vol. 217, no. January, p. 108090, 2020, doi: 10.1016/j.oceaneng.2020.108090.

[15] A. Hosseini and N. Goudarzi, "Design and CFD study of a hybrid vertical-axis wind turbine by employing a combined Bach-type and H-Darrieus rotor systems," *Energy Convers. Manag.*, vol. 189, pp. 49–59, 2019, doi: 10.1016/j.enconman.2019.03.068.

[16] P. M. Kumar, K. Sivalingam, S. Narasimalu, T.-C. Lim, S. Ramakrishna, and H. Wei, "A Review on the evolution of Darrieus vertical axis wind turbine: Small wind turbines," *J. Power Energy Eng.*, vol. 07, no. 04, pp. 27–44, 2019, doi: 10.4236/jpee.2019.74002.

[17] M. J. Alam and M. T. Iqbal, "A low cut-in speed marine current turbine," *J. Ocean Technol.*, vol. 5, no. 4, pp. 49–62, 2010.

[18] W. H. Lam and L. Chen, "Equations used to predict the velocity distribution within a wake from a horizontal-axis tidal-current turbine," *Ocean Eng.*, vol. 79, pp. 35–42, 2014, doi: 10.1016/j.oceaneng.2014.01.005.

[19] P.A.S.F. Silva, T.F. De Oliveira, A.C.P. Brasil Junior, and J.R.P. Vaz, "Numerical study of wake characteristics in a horizontal-axis Hydrokinetic turbine," *An. Acad. Bras. Cienc.*, vol. 88, no. 4, pp. 2441–2456, 2016, doi: 10.1590/0001-3765201620150652.

[20] R.E. Bensow, C. Fureby, M. Liefvendahl, T. Persson, "A comparative study of RANS, DES and LES," *26th ONR Symp. Nav. Hydrodyn.*, vol. 2, pp. 17–22, 2006.

[21] N. Mulvany, L. Chen, J. Tu, and B. Anderson, "Steady-state evaluation of two-equation RANS (Reynolds-Averaged Navier-Stokes) turbulence models for high-reynolds number hydrodynamic flow simulations," *Dep. Defence, Aust.Gov.*, pp.1–54,2004, Available:http://oai.dtic.mil/oai/oai?verb=getRecord&metadataPrefix=html&identifier=ADA426359.

[22] A. Rahman, N. B. Yahaya, and M. T. A. Rahman, "The effect of support structure on RANS actuator disc for shallow water application," *IOP Conf. Ser. Mater. Sci. Eng.*, vol. 670, no. 1, 2019, doi: 10.1088/1757-899X/670/1/012078.

[23] S. M. Rassoulinejad-Mousavi, M. Jamil, and M. Layeghi, "Experimental study of a combined three bucket H-rotor with savonius wind turbine," *World Appl. Sci. J.*, vol. 28, no. 2, pp. 205–211, 2013, doi: 10.5829/idosi.wasj.2013.28.02.1429.

[24] A. Bakri, "Numerical assessment of vertical axis marine current turbines performances in shallow water : A case study for Malaysia," 2020.

[25] E. M. Alawadhi, "Meshing guide," *Finite Elem. Simulations Using ANSYS*, 2nd Edition, CRC Press, 2015.

[26] G.E Suhri, A. Rahman, L. Dass, K. Rajendran, "The influence of Tidal turbine in arrangement on the wake interaction in shallow water.," *Journal of Physics: Conference Series*, no. 2051 012058, 2021.

[27] M. E. Harrison, W. M. J. Batten, L. E. Myers, and A. S. Bahaj, "Comparison between CFD simulations and experiments for predicting the far wake of horizontal axis tidal turbines," *IET Renew. Power Gener.*, vol. 4, no. 6, pp. 613–627, 2010, doi: 10.1049/iet-rpg.2009.0193.

[28] K. Rogowski, M. O. L. Hansen, and G. Bangga, "Performance analysis of a H-darrieus wind turbine for a series of 4-digit NACA airfoils," *Energies*, vol. 13, no. 12, 2020, doi: 10.3390/en13123196.

[29] B. K. Kirke and L. Lazauskas, "Limitations of fixed pitch Darrieus hydrokinetic turbines and the challenge of variable pitch," *Renew. Energy*, vol. 36, no. 3, pp. 893–897, 2011, doi: 10.1016/j.renene.2010.08.027.

[30] G. Erfort, T. W. von Backstrm, and G. Venter, "Reduction in the torque ripple of a vertical axis wind turbine through coupled optimization of the pitch angle," *11th South African Conf. Comput. Appl. Mech. SACAM 2018*, 17-18 Sept., South Africa, 2018.